Pathology - Research and Practice 215 (2019) 152665

Contents lists available at ScienceDirect

Pathology - Research and Practice

journal homepage: www.elsevier.com/locate/prp

Case report

Ewing sarcoma with myxoid stroma: Case report of an unusual histological variant

Borislav A. Alexiev*, Farres Obeidin, Lawrence J. Jennings

Department of Pathology, Northwestern University Feinberg School of Medicine, Northwestern Memorial Hospital, 251 East Huron St, Feinberg 7-342A, Chicago, IL 60611, United States

ARTICLE INFO

Keywords:
Ewing sarcoma
Myxoid variant
EWSR1-FLI1 fusion transcript

ABSTRACT

We describe the case of a Ewing sarcoma with prominent myxoid stroma of the temporal bone in a 26-year-old female. Histologically, the tumor exhibited a fascicular growth pattern of round to spindled cells with a minimal amount of pale eosinophilic to clear cytoplasm and oval or spindled nuclei with finely dispersed chromatin and small nucleoli. Myxoid changes were prominent (> 50%), with reticular or pseudoacinar growth of the loosely cohesive cells. The tumor showed strong expression of CD99, FLI1, and CD56 and was positive for the EWSR1-FLI1 fusion transcript. The diagnosis of Ewing sarcoma with myxoid stroma (myxoid variant) is particularly problematic owing to the large number of potential mimics. The tumor extends the morphologic spectrum of Ewing sarcoma beyond the previously described histological variants, and broadens the differential diagnosis. For any round/spindle cell sarcoma, prominent myxoid stroma and CD99 immunoreactivity should prompt consideration for molecular studies that include analysis of both *EWSR1* and *FLI1*.

1. Introduction

The Ewing sarcoma family of tumors (ESFT) is a group of malignant small round blue cell tumors (SRBCT) that includes Ewing sarcoma (ES) of bone, extra-osseous ES, primitive neuroectodermal tumors (PNET), and Askin tumor (PNET of the chest wall) [2,3,6,7,15]. These tumors are considered to be derived from a common cell of origin and primarily affects the pediatric and young adult population. The pathological diagnosis of ESFT is based on the finding of a SRBCT that stains for CD99 and expresses one of several reciprocal translocations, most commonly t (11;22)(q24;q12) between the amino-terminus of the *EWSR1* gene and the carboxy-terminus of the *FLI1* gene found in 85–90% of cases [2,3,6,7,15]. Atypical ES are the most challenging of the ESFT subtypes since the differential diagnosis with other SRBCT of bone and soft tissue is broad. [6,17]. Precise tumor classification is crucial for establishing prognosis and in guiding appropriate therapeutic strategies. Judging by the published literature, ESFT with atypical features involving the head and neck are extremely rare [2,3,6,7,15,17]. We present a diagnostically challenging case of ES with prominent myxoid stroma arising in the temporal bone of a 26-year-old female. To the best of our knowledge, a myxoid variant of ES has not been previously described.

2. Clinical history

A 26-year-old female with no significant past medical history presented to the neurosurgical clinic because of an incidentally discovered right temporal bone lesion during a workup for headaches. She denied any symptoms and clinical examination showed no neurological findings. Computed tomography showed a 4.3 cm expansile, lytic, and well-corticated lesion centered in the squamous portion of the right temporal bone (Fig. 1A). Magnetic resonance imaging demonstrated an expansile lesion with heterogenous T2 signal enhancement. Subtle hyperenhancement of the overlying dura and moderate mass effect on the temporal lobe was seen (Fig. 1B). The radiographic differential diagnosis included an intra-osseous meningioma, atypical fibrous dysplasia, and hemangioma. Malignancy was deemed less likely.

3. Materials and methods

Representative tissue sections from the temporal bone mass were fixed in 10% buffered formalin and embedded in paraffin after decalcification. Representative tissue blocks were submitted for frozen section and permanent sections. For routine microscopy, 4-μm-thick sections were stained with hematoxylin-eosin (H&E). Immunohistochemical staining was performed using an automated immunostainer (Leica Bond-III, Leica Biosystems, Buffalo Grove, IL)

* Corresponding author.
E-mail address: Borislav.Alexiev@northwestern.edu (B.A. Alexiev).

https://doi.org/10.1016/j.prp.2019.152665
Received 15 July 2019; Received in revised form 20 September 2019; Accepted 21 September 2019

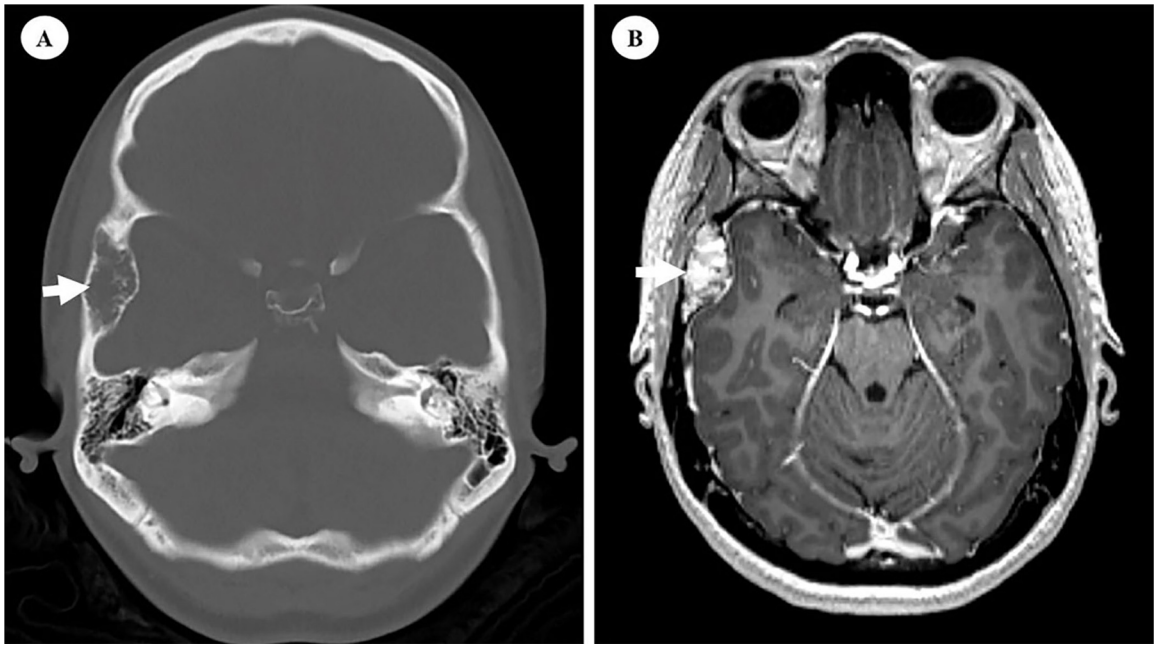

Fig. 1. A. Ewing sarcoma with myxoid stroma. Note expansile, lytic, well-corticated lesion (arrow) centered in the squamous portion of the right temporal bone. Computed tomography. B. Ewing sarcoma with myxoid stroma. Note expansile lesion (arrow) with heterogenous T2 signal enhancement. Subtle hyperenhancement of the overlying dura and moderate mass effect on the temporal lobe is seen. Magnetic resonance imaging.

Table 1
List of primary antibodies used in the study.

Antibody Name	Manufacturer	Species	Clone	Dilution
AE1/AE3	Dako	Mouse	AE1/AE3	1:200
CD31	Leica	Mouse	JC70A	Predilute
CD56	Leica	Mouse	CD564	Predilute
CD99	Ventana	Mouse	O13	Predilute
Desmin	Ventana	Mouse	DE-R-11	Predilute
EMA	Ventana	Mouse	E29	Predilute
ERG	Abcam	Mouse	EPR3864	Predilute
FLI-1	Cell Marque	Mouse	MRQ-1	Predilute
Ki-67	Ventana	Rabbit	30-9	Predilute
MUC4	Epitomics	Rabbit	EP256	1:20
MyoD1	Cell Marque	Rabbit	EP212	Predilute
S100	Ventana	Mouse	4C4.9	Predilute
SOX10	Cell Marque	Rabbit	EP268	Predilute
SSTR2A	Abcam	Mouse	UMB1	1:250
STAT6	Santa Cruz	Mouse	D-1	1:1000
WT-1	Leica	Mouse	WT49	Predilute

and BondRefinePolymerTM biotin-free DAB detection kit. The antibodies applied in the study are listed in Table 1. A positive nuclear, cytoplasmic and/or membranous expression in 10% or more of neoplastic cells qualified as "positive (+)".

Molecular genetic studies were performed at Lurie Children's Hospital on formalin-fixed, paraffin-embedded tumor tissue using reverse transcriptase polymerase chain reaction (RT-PCR). Total RNA was extracted from 2 unstained formalin-fixed paraffin embedded tissue sections on glass slides (5-micron sections). The extracted RNA was reverse transcribed in duplicate to cDNA with reverse transcriptase. The cDNA was subsequently analyzed as multiple singleplex assays using primers specific to *EWSR1-FLI1* fusion transcripts (exon 7 to exon 5 and exon 7 to exon 6 variants), *EWSR1-ERG* (exon 7 to exon 6 variants), *CIC-DUX4* fusion transcripts [10,11]. Two primer sets specific to Ewing-like sarcoma *BCOR-CCNB3* (exon 15 to exon 5) fusion transcripts were also used [21], as well as primers specific to the *SYT-SSX1*, *SYT-SSX2*, *SYT-SSX4*, *SYT-SSX7*, and *SYT-SSX8* fusion transcripts. Products were analyzed using real-time PCR and melt curve analysis. The quality of the mRNA was assessed by an independent amplification of a larger product, the ubiquitously expressed *GUSB* mRNA.

Sanger sequencing assay was used to confirm the RT-PCR results. To remove unused dNTPs and primers left over from the RT-PCR reaction, 10 µl of amplicon was transferred to a new PCR tube and 1 µl of ExoSAP-IT® (Affimetrix, Santa Clara, CA) was added. The amplicon clean-up was preformed following ExoSAP-IT® manufacture instructions. 2 µl of the cleaned product was used for sequencing reactions with the "Big Dye Terminator v1.1 Cycle Sequencing" kit (Life Technologies, Carlsbad, CA) by the M13 forward primer 5′ - TGT AAA ACG ACG GCC AGT - 3′ and reverse primer 5′ - CAG GAA ACA GCT ATG ACC - 3′, in an ABI Prism 3130 xl automatic sequencer (Life Technologies, Carlsbad, CA) in both directions. Data were analyzed by Mutation Surveyor (SoftGenetics, State College, PA).

4. Results

4.1. Histology and immunohistochemical findings

Histologically, the tumor consisted of vague nodular aggregates of uniform spindled and rounded cells arranged in short fascicles (Fig. 2A and B). Reticular and pseudoacinar structures within the more myxoid areas could be seen that accounted for more than 50% of the tumor volume (Fig. 2C and D). The tumor cells exhibited oval to spindle nuclei with finely dispersed chromatin, small nucleoli, and pale eosinophilic to clear cytoplasm (Fig. 3A). The primary tumor mitotic rate was 2 mitoses/10 high power fields. No tumor necrosis was identified.

The immunohistochemical diagnostic panel showed strong expression of CD99 (membranous), FLI1, and CD56 in the tumor (Fig. 3B–D) while somatostatin receptor 2 (SSTR2A), STAT6, CD31, S100, SOX10, AE1/AE3, EMA, ERG, MUC4, myoD1, WT1, and desmin immunostains were negative. The Ki67 proliferative index was < 10%.

4.2. Molecular genetic studies

The tumor cells were positive for the *EWSR1-FLI1* fusion transcript. No *CIC-DUX4*, *BCOR-CCNB3*, *SYT-SSX1*, *SYT-SSX2*, *SYT-SSX4*, *SYT-SSX7*, or *SYT-SSX8* fusion transcripts were identified. Bidirectional Sanger dideoxy sequencing of the RT-PCR product confirmed the

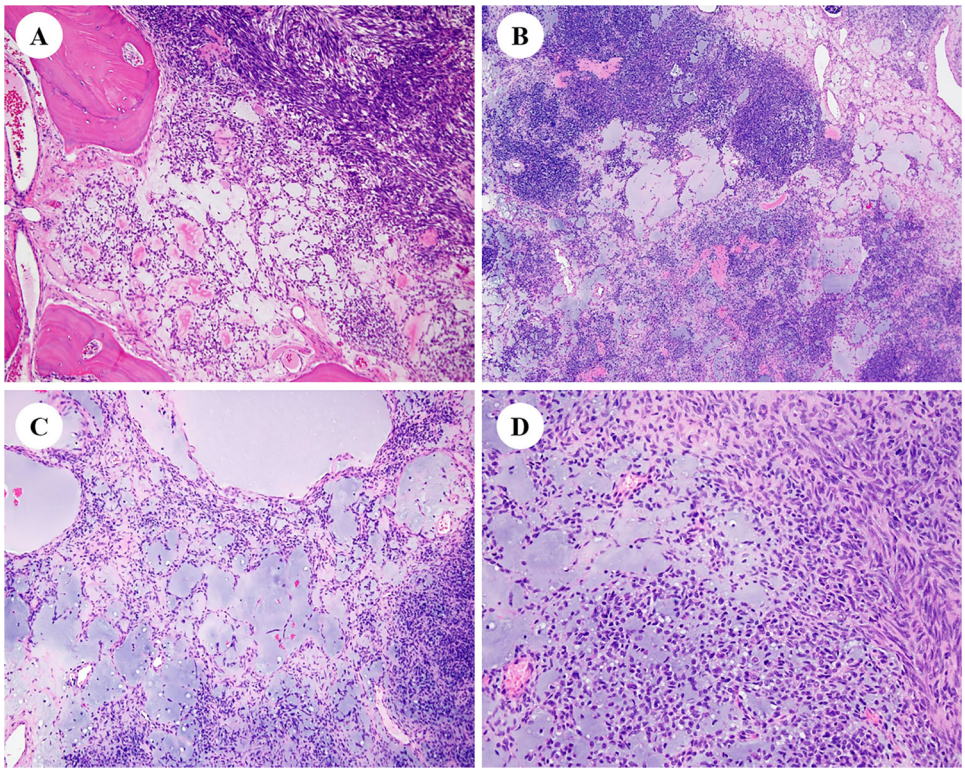

Fig. 2. A and B. Ewing sarcoma with myxoid stroma. Vague nodular aggregate of uniform spindled cells forming short fascicles and reticular growth of cells in more myxoid areas. Note bone invasion in Fig. 2A. H&E stain, 100x (Fig. 2A) and 40x (Fig. 2B). C and D. Ewing sarcoma with myxoid stroma. Note anastomosing corded (reticular) pattern of cells in a myxoid stroma. H&E stain, 100x (Fig. 2C) and 200x (Fig. 2D).

presence of the EWSR1 (exon 7) to FLI1 (exon 6) fusion transcript (Fig. 4).

4.3. Overall treatment plan

The patient underwent a right temporal craniectomy for resection of the bone mass. Following diagnosis, the patient began treatment with chemotherapy and is planned for seven cycles of vincristine, doxorubicin, and cyclophosphamide alternating with seven cycles of ifosfamide and etoposide.

5. Discussion

Primary ES of the head and neck is uncommon [2]. Atypical ES,

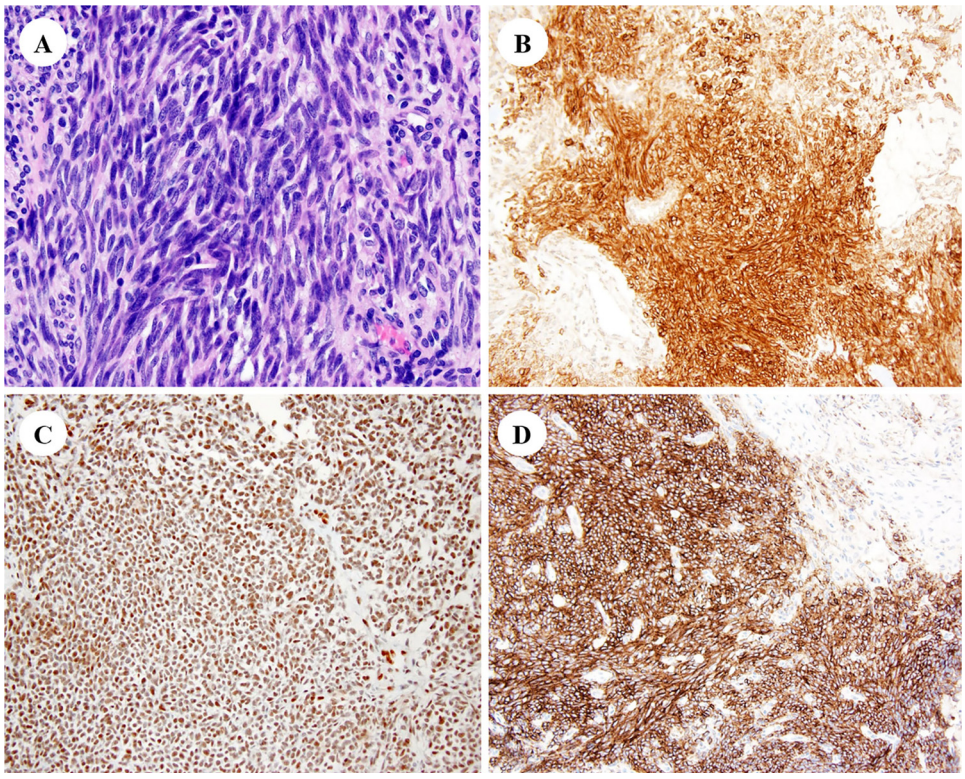

Fig. 3. A. Ewing sarcoma with myxoid stroma. Note oval-to-spindle nuclei with finely dispersed chromatin and small nucleoli, and pale eosinophilic to clear cytoplasm. H&E stain, 400 × . B. Ewing sarcoma with myxoid stroma. CD99 stain is strongly positive in tumor cells. CD99 stain, 200 × . C. Ewing sarcoma with myxoid stroma. FLI1 stain is strongly positive in tumor cells. FLI1 stain, 200 × . D. Ewing sarcoma with myxoid stroma. CD56 stain is strongly positive in tumor cells. CD56 stain, 200 × .

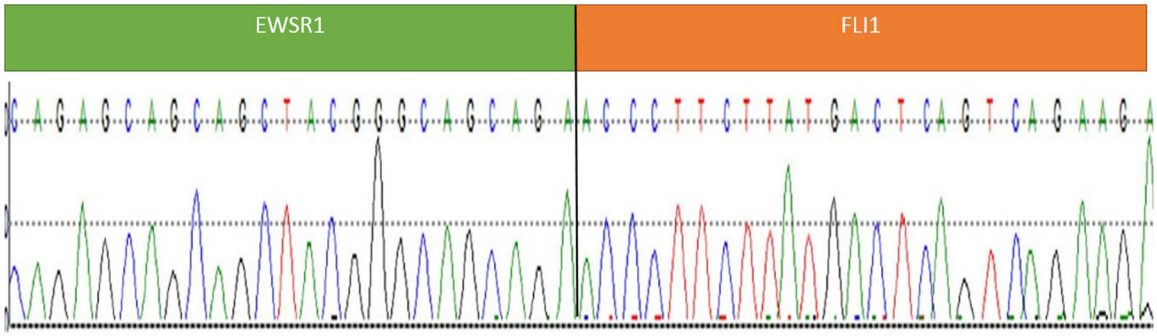

Fig. 4. Ewing sarcoma with myxoid stroma. Sanger sequencing of the RT-PCR product confirms the presence of the EWSR1 (exon 7) to FLI1 (exon 6) fusion transcript.

including adamantinoma-like, spindled, sclerosing, and clear cell/anaplastic variants, are the most challenging of the ESFT subtypes [2,6,15,17]. Prominent myxoid change has not been previously observed in pre-treatment *EWSR1-FLI1* rearranged ES.

We present a challenging case of ES centered in the temporal bone of a 26-year-old female. The tumor exhibited a fascicular growth pattern of cells with minimal pale eosinophilic to clear cytoplasm and oval-to-spindle nuclei with finely dispersed chromatin and small nucleoli. Myxoid changes were prominent (> 50%), with reticular and pseudoacinar arrangement of the loosely cohesive small round and spindle cells. Immunohistochemical and molecular studies demonstrated CD99 and FLI1 expression and the presence of a *EWSR1-FLI1* fusion transcript. The tumor was classified as ES, myxoid variant.

The differential diagnosis of ES with prominent myxoid stroma is broad and includes numerous primitive tumors with myxoid features arising in this location, such as *CIC-DUX4* and *BCOR-CCNB3* fusion-gene-associated small round cell sarcoma (SRCS), myoepithelial tumors, myxoid chondrosarcoma, *EWSR1-NFATC2* fusion-gene-associated sarcoma, synovial sarcoma, and malignant peripheral nerve sheath tumor (MPNST).

A histologic comparison of the *CIC-DUX4* fusion-gene-associated SRCS with classic *EWSR1*-rearranged ES shows lobular growth pattern, necrosis, significantly higher degrees of nuclear pleomorphism, prominent nucleoli, and spindle cell elements in the former [4,9–11,24,25]. Diffuse ETV4 along with at least focal WT1 expression and negative NKX2.2 is helpful to distinguish *CIC-DUX4* fusion-gene-associated sarcoma from ES and other histologic mimics [9].

BCOR-CCNB3 fusion-gene-associated SRCS are generally composed of aggregates of short spindled and rounded tumor cells with vesicular nuclei, finely dispersed chromatin, inconspicuous nucleoli and an arciform vascular pattern [16,21,24]. Distinguishing immunohistochemical features include CCNB3 reactivity and expression of SATB2 and Pax8 in more than 50% of cases [14,16].

A round cell/undifferentiated form of myoepithelial carcinoma of either salivary gland or soft tissue may also be difficult to distinguish from myxoid ES [18]. Both tumors may exhibit nuclear uniformity, clear cytoplasm, eosinophilic matrix-like material or myxoid stroma, and immunostaining for the CD99, keratins, and S100 protein [2]. However, myoepithelial carcinoma is FLI1 immunonegative [22]. The similarities extend at the molecular level, because soft tissue myoepithelial tumors often harbor rearrangements of *EWSR1*. As such, demonstration of the *EWSR1* rearrangement by itself is not sufficient for a definitive diagnosis of myxoid ES. In unconventional cases, it is indispensable to reveal the fusion partner gene – *FLI1* for myxoid ES and *POU5F1, PBX1, PBX3, or ZNF444* for myoepithelial carcinoma – for a more definitive classification [1,2,22].

EWSR1-NFATC2 fusion-gene-associated sarcoma is a novel bone and soft tissue tumor with immunomorphologic overlap with ES, myoepithelial tumors, and extraskeletal myxoid chondrosarcoma [18,23]. Most tumors show monomorphic round to epithelioid cells in anastomosing cords and abundant myxohyaline to collagenous extracellular matrix. The tumor stains for CD99 and NKX2.2, while EMA, dot-like cytokeratin, WT1, and SMA may also be present [23]. *EWSR1-NFATC2* fusion-gene-associated sarcoma is resistant to ES-specific chemotherapy [23].

Myxoid synovial sarcoma exhibits epithelial differentiation by light microscopy and immunohistochemistry and is frequently CD99 positive [5,12]. TLE1 is a sensitive and specific marker for synovial sarcoma and can be helpful in distinguishing synovial sarcoma from its histological mimics. Molecular confirmation of translocations involving the *SYT* gene remains the gold standard.

Extraskeletal myxoid chondrosarcoma is a malignant mesenchymal neoplasm of uncertain differentiation [8,19]. The neoplasm demonstrates lobulated architecture with uniform round to spindled cells forming interconnecting cords, clusters, or trabeculae in a background of myxoid matrix. An extensive fibrosarcoma-like spindle cell component may be present. Extraskeletal myxoid chondrosarcomas express INSM1 in 90% of cases [26]. A subset of tumors is positive for S100, CD117, synaptophysin, and neuron-specific enolase. Recurrent gene fusions involving *NR4A3* on chromosome 9 are observed in the majority of extraskeletal myxoid chondrosarcomas. The most common fusion partner is *EWSR1*, resulting in t(9;22)(q22;q12) [8,19].

The diagnosis of head and neck MPNST is particularly challenging to distinguish from other spindle cell sarcoma types outside the neurofibromatosis type 1 (NF1) context [13,20]. The tumor is composed of spindle cells arranged in sweeping fascicles. Dense cellular areas alternate with hypocellular, myxoid zones, imparting a “marbled” appearance. MPNSTs lack a specific immunohistochemical profile, with the traditional neural markers such as S100 protein and SOX10 having suboptimal sensitivity and specificity [13,20]. Recent studies demonstrated inactivation of the different components of polycomb repressive complex 2 (PRC2) through mutations of *EED* or *SUZ12* in the majority of MPNST [20]. Homozygous inactivation of PRC2 leads to loss of trimethylation at lysine 27 of histone 3 (H3K27me3) on immunohistochemical analysis, which has become a reliable diagnostic marker in distinguishing MPNST from histologic mimics [13,20]. Compared to other molecularly confirmed subsets of head and neck sarcomas (ES, Ewing-like sarcoma, rhabdomyosarcoma and synovial sarcoma), high grade MPNST have the worst overall survival [13].

6. Conclusion

The tumor extends the morphologic spectrum of ES beyond the previously described histological variants, and broadens the differential diagnosis. For any round/spindle cell sarcoma, prominent myxoid stroma and CD99 immunoreactivity should prompt consideration for molecular studies that include analysis of both *EWSR1* and *FLI1*. Recognition of the myxoid variant of ES is important because it can easily be mistaken for other myxoid neoplasms, potentially resulting in suboptimal therapy. The overall survival of patients with ES is

significantly better than that for patients with *CIC-DUX4* and *BCOR-CCNB3* fusion-gene-associated SRCS [19/24, 20/25].

Funding

No external funds were obtained for this work.

Declaration of Competing Interest

We declare that we have no conflict of interest.

References

[1] C.R. Antonescu, L. Zhang, N.E. Chang, B.R. Pawel, W. Travis, N. Katabi, M. Edelman, A.E. Rosenberg, G.P. Nielsen, P. Dal Cin, C.D. Fletcher, EWSR1-POU5F1 fusion in soft tissue myoepithelial tumors. A molecular analysis of sixty-six cases, including soft tissue, bone, and visceral lesions, showing common involvement of the EWSR1 gene, Genes Chromosom. Cancer 49 (2010) 1114–1124.

[2] J.A. Bishop, R. Alaggio, L. Zhang, R.R. Seethala, C.R. Antonescu, Adamantinoma-like Ewing family tumors of the head and neck: a pitfall in the differential diagnosis of basaloid and myoepithelial carcinomas, Am. J. Surg. Pathol. 39 (2015) 1267–1274.

[3] J.A. Bridge, M.E. Fidler, J.R. Neff, J. Degenhardt, M. Wang, C. Walker, H.D. Dorfman, K.S. Baker, T.A. Seemayer, Adamantinoma-like Ewing's sarcoma: genomic confirmation, phenotypic drift, Am. J. Surg. Pathol. 23 (1999) 159–165.

[4] E.Y. Choi, D.G. Thomas, J.B. McHugh, R.M. Patel, D. Roulston, S.M. Schuetze, R. Chugh, J.S. Biermann, D.R. Lucas, Undifferentiated small round cell sarcoma with t(4;19)(q35;q13.1) CIC-DUX4 fusion: a novel highly aggressive soft tissue tumor with distinctive histopathology, Am. J. Surg. Pathol. 37 (2013) 1379–1386.

[5] A. Coli, G. Bigotti, R. Parente, G. Massi, Myxoid monophasic synovial sarcoma: case report of an unusual histological variant, J. Exp. Clin. Cancer Res. 25 (2006) 287–291.

[6] A.L. Folpe, J.R. Goldblum, B.P. Rubin, B.M. Shehata, W. Liu, A.P. Dei Tos, S.W. Weiss, Morphologic and immunophenotypic diversity in Ewing family tumors: a study of 66 genetically confirmed cases, Am. J. Surg. Pathol. 29 (2005) 1025–1033.

[7] S. Hafezi, R.R. Seethala, E.B. Stelow, S.E. Mills, I.T. Leong, E. MacDuff, J.L. Hunt, B. Perez-Ordoñez, I. Weinreb, Ewing's family of tumors of the sinonasal tract and maxillary bone, Head Neck Pathol. 5 (2011) 8–16.

[8] M. Hisaoka, H. Hashimoto, Extraskeletal myxoid chondrosarcoma: updated clinicopathological and molecular genetic characteristics, Pathol. Int. 55 (2005) 453–463.

[9] Y.P. Hung, C.D. Fletscher, J.L. Hornick, Evaluation of ETV4 and WT1 expression in CIC-rearranged sarcomas and histologic mimics, Mod. Pathol. 29 (2016) 1324–1334.

[10] A. Italiano, Y.S. Sung, L. Zhang, S. Singer, R.G. Maki, J.M. Coindre, C.R. Antonescu, High prevalence of CIC fusion with double-homeobox (DUX4) transcription factors in EWSR1-negative undifferentiated small blue round cell sarcomas, Genes Chromosom. Cancer 51 (2012) 207–218.

[11] M. Kawamura-Saito, Y. Yamazaki, K. Kaneko, N. Kawaguchi, H. Kanda, H. Mukai, T. Gotoh, T. Motoi, M. Fukayama, H. Aburatani, T. Takizawa, T. Nakamura, Fusion between CIC and DUX4 up-regulates PEA3 family genes in Ewing-like sarcomas with t(4;19)(q35;q13) translocation, Hum. Mol. Genet. 15 (2006) 2125–2137.

[12] J.F. Krane, F. Bertoni, C.D. Fletcher, Myxoid synovial sarcoma: an underappreciated morphologic subset, Mod. Pathol. 12 (1999) 456–462.

[13] S. Le Guellec, A.V. Decouvelaere, T. Filleron, I. Valo, C. Charon-Barra, Y.M. Robin, P. Terrier, C. Chevreau, J.M. Coindre, Malignant peripheral nerve sheath tumor is a challenging diagnosis: a systematic pathology review, immunohistochemistry, and molecular analysis in 160 patients from the French sarcoma group database, Am. J. Surg. Pathol. 40 (2016) 896–908.

[14] W.S. Li, I.C. Liao, M.C. Wen, H.H. Lan, S.C. Yu, H.Y. Huang, BCOR-CCNB3 positive soft tissue sarcoma with round-cell and spindle-cell histology: a series of four cases highlighting the pitfall of mimicking poorly differentiated synovial sarcoma, Histopathology 69 (2016) 792–801.

[15] A. Llombart-Bosch, I. Machado, S. Navarro, F. Bertoni, P. Bacchini, M. Alberghini, A. Karzeladze, N. Savelov, S. Petrov, I. Alvarado-Cabrero, D. Mihaila, P. Terrier, J.A. Lopez-Guerrero, P. Picci, Histological heterogeneity of Ewing's sarcoma/PNET: an immunohistochemical analysis of 415 genetically confirmed cases with clinical support, Virch. Arch. 455 (2009) 397–411.

[16] K. Ludwig, R. Alaggio, A. Zin, M. Peron, V. Guzzardo, S. Benini, A. Righi, M. Gambarotti, BCOR-CCNB3 undifferentiated sarcoma – does immunohistochemistry help in the identification? Pediatr. Dev. Pathol. 20 (2017) 321–329.

[17] I. Machado, R. Noguera, E.A. Mateos, S. Calabuig-Fariñas, F.I. López, A. Martínez, S. Navarro, A. Llombart-Bosch, The many faces of atypical Ewing's sarcoma. A true entity mimicking sarcomas, carcinomas and lymphomas, Virch. Arch. 458 (2011) 281–290.

[18] M. Miettinen, A. Felisiak-Golabek, A. Luina Contreras, J. Glod, R.N. Kaplan, J.K. Killian, J. Lasota, New fusion sarcomas: histopathology and clinical significance of selected entities, Hum. Pathol. 86 (2019) 57–65.

[19] A.M. Oliveira, T.J. Sebo, J.E. McGrory, T.A. Gaffey, M.G. Rock, A.G. Nascimento, Extraskeletal myxoid chondrosarcoma: a clinicopathologic, immunohistochemical, and ploidy analysis of 23 cases, Mod. Pathol. 13 (2000) 900–908.

[20] A.A. Owosho, C.L. Estilo, J.M. Huryn, P. Chi, C.R. Antonescu, A clinicopathologic study of head and neck malignant peripheral nerve sheath tumors, Head Neck Pathol. 12 (2018) 151–159.

[21] G. Pierron, F. Tirode, C. Lucchesi, S. Reynaud, S. Ballet, S. Cohen-Gogo, V. Perrin, J.M. Coindre, O. Delattre, A new subtype of bone sarcoma defined by BCOR-CCNB3 gene fusion, Nat. Genet. 44 (2012) 461–466.

[22] B. Rekhi, S. Joshi, Y. Panchwagh, A. Gulia, A. Borges, J. Bajpai, N.A. Jambehekar, V. Pant, M. Mandholkar, S. Byregowda, A. Puri, Clinicopathological features of five unusual cases of intraosseous myoepithelial carcinomas, mimicking conventional primary bone tumours, including EWSR1 rearrangement in one case, APMIS 124 (2016) 278–290.

[23] G.Y. Wang, D.G. Thomas, J.L. Davis, T. Ng, R.M. Patel, P.W. Harms, B.L. Betz, S.M. Schuetze, J.B. McHugh, A.E. Horvai, S.J. Cho, D.R. Lucas, EWSR1-NFATC2 translocation-associated sarcoma clinicopathologic findings in a rare aggressive primary bone or soft tissue tumor, Am. J. Surg. Pathol. 43 (2019) 1112–1122.

[24] Y. Yamada, M. Kuda, K. Kohashi, H. Yamamoto, J. Takemoto, T. Ishii, K. Iura, A. Maekawa, H. Bekki, T. Ito, H. Otsuka, M. Kuroda, Y. Honda, S. Sumiyoshi, T. Inoue, N. Kinoshita, A. Nishida, K. Yamashita, I. Ito, S. Komune, T. Taguchi, Y. Iwamoto, Y. Oda, Histological and immunohistochemical characteristics of undifferentiated small round cell sarcomas associated with CIC-DUX4 and BCOR-CCNB3 fusion genes, Virch. Arch. 470 (2017) 373–380.

[25] A. Yoshida, K. Goto, M. Kodaira, E. Kobayashi, H. Kawamoto, T. Mori, S. Yoshimoto, O. Endo, N. Kodama, R. Kushima, N. Hiraoka, T. Motoi, A. Kawai, CIC-rearranged sarcomas: a study of 20 cases and comparisons with Ewing sarcomas, Am. J. Surg. Pathol. 40 (2016) 313–323.

[26] A. Yoshida, N. Makise, S. Wakai, A. Kawai, N. Hiraoka, INSM1 expression and its diagnostic significance in extraskeletal myxoid chondrosarcoma, Mod. Pathol. 31 (2018) 744–752.